Original Article

Transcriptome analysis of induced pluripotent stem cells' osteogenic differentiation reveals NPY1R activating PI3K/AKT/mTOR in alveolar bone loss during periodontitis

Xiaowen Li^{1*}, Ruikang Guo^{2*}, Lingling Liang¹, Hao Liang¹, Guangqi Zhou¹, Qinglan Lu¹, Yonghui Huang¹, Zhen Qi², Xiaojie Li¹

¹Guangxi Key Laboratory of Oral and Maxillofacial Rehabilitation and Reconstruction, College and Hospital of Stomatology, Guangxi Medical University, Nanning 530021, Guangxi, P. R. China; ²Department of Cardiovascular Surgery, The Second Xiangya Hospital, Central South University, Changsha 410000, Hunan, P. R. China. *Equal contributors.

Received January 31, 2025; Accepted September 11, 2025; Epub October 15, 2025; Published October 30, 2025

Abstract: Objective: Periodontitis, a prevalent oral disease leading to alveolar bone defects, remains a primary cause of tooth loss in adults. The biologic mechanisms driving bone loss in periodontitis are still poorly understood, limiting the development of genetic treatment. This study investigates potential therapeutic targets for alveolar bone loss by analyzing transcriptomic data related to the osteogenic differentiation of induced pluripotent stem cells (iPSCs). Methods: Using *in vitro* and *in vivo* models, we examined the role of neuropeptide Y receptor Y1 (NPY1R) and the PI3K-AKT-mTOR (PAM) signaling pathway in osteogenic differentiation and bone loss. A combination of bioinformatics, molecular biology, and histologic techniques was employed to pinpoint key signaling events that influence bone remodeling in periodontitis and to identify potential intervention points. Results: Transcriptomic profiling during iPSC osteogenic differentiation revealed significant upregulation of neuropeptide Y (NPY) and NPY1R. Suppression of NPY1R reduced the osteogenic capacity of iPSCs. Activation of the PAM pathway was observed during osteogenesis, and treatment with LY294002, a PAM pathway inhibitor, led to decreased osteogenic activity. *In vivo* experiments using a rat periodontitis model confirmed increased expression of NPY1R and activation of the PAM pathway, suggesting a role in bone repair processes. Conclusion: The NPY/NPY1R axis and the PAM signaling pathway appear to regulate bone regeneration and may be involved in preventing alveolar bone loss in periodontitis. These findings provide a new direction for therapy targeting bone defects associated with periodontal disease.

Keywords: iPS cell, bioinformatics analysis, NPY1R, PI3K/mTOR pathway, periodontitis, therapeutic target

Introduction

Periodontitis ranks among the most widespread oral diseases [1]. Its chronic and progressive inflammatory nature can lead to alveolar bone defects [2], often resulting in tooth loss and impaired mastication [3]. Bacteria associated with periodontitis may enter the systemic circulation, where they can trigger or worsen conditions such as cardiovascular disease, cerebrovascular disorders, and diabetes [4]. The pathophysiology of periodontitis involves intricate interactions between periodontal pathogens, host immune defenses, and locally produced inflammatory mediators [5]. More

recently, research has shown that disruptions in bone remodeling contribute significantly to disease progression [6]. Bone remodeling is a continuous and tightly regulated process requiring coordination between osteoclastic bone resorption and osteoblastic bone formation. Under normal physiologic conditions, this balance maintains the integrity and function of bone tissue. In periodontitis, however, this equilibrium is frequently disturbed, giving rise to bone destruction.

Although numerous molecular mechanisms aimed at preventing alveolar bone loss in periodontitis have been proposed [2], relatively

few studies have examined early developmental processes to identify therapeutic targets. Induced pluripotent stem cells (iPSCs) represent a promising model for investigating osteogenic differentiation and bone-related disorders. Their patient-specific nature allows for detailed exploration of disease mechanisms at both the cellular and molecular levels [7]. In this study, we applied transcriptome sequencing to an iPSC-derived osteogenic differentiation model to analyze molecular pathways associated with alveolar bone loss in periodontitis, with the goal of identifying possible treatment strategies.

Neuropeptide Y1 receptor (NPY1R) plays a key role in regulating bone formation [8]. Prior work has demonstrated that NPY1R activation can stimulate osteogenesis by controlling the proliferation, differentiation, and function of osteoblasts. Specifically, NPY facilitates the secretion of bone matrix components and boosts mineralization in osteoblasts by binding to NPY1R [9]. Beyond direct effects on osteoblasts, NPY1R may also influence bone health indirectly by affecting local inflammation and vascular supply, which are critical for maintaining bone tissue. Despite its potential biological and therapeutic relevance in bone remodeling and regeneration, the roles of NPY and NPY1R in periodontitis-related bone defects remain uninvestigated.

In this study, we identified changes in the expression levels of NPY and NPY1R before and after osteogenic differentiation, based on transcriptome sequencing data from an induced pluripotent stem cell model of osteogenesis [10]. Activation of the NPY/NPY1R axis influenced key signaling pathways, particularly the phosphoinositide 3-kinase (PI3K)/mechanistic target of rapamycin (mTOR) pathway [11], which plays a central role in regulating cell survival, growth, and proliferation. Disruptions in the PI3K/mTOR pathway have been observed in a range of bone-related conditions, including osteoporosis and periodontitis [12]. By examining the involvement of NPY and NPY1R in these processes, we aim to identify therapeutic targets for preventing and treating bone loss associated with periodontitis. This work advances our understanding of the relationship between neuropeptides and bone metabolism, and it opens new directions for therapy of periodontal disease.

Materials and methods

Acquistion of data

Genomic sequences were obtained from the GSE219215 dataset in the Gene Expression Omnibus (GEO). Raw count data were used for differential expression analysis. This analysis was performed with the DESeq2 R package (version 1.4.5). Genes were considered differentially expressed when $|\log 2(\text{Fold change})| \ge 2$ and P < 0.05.

Bioinformatic analysis

Subsequent analyses included heatmap clustering, Principal Component Analysis (PCA), volcano plot generation, Gene Set Enrichment Analysis (GSEA), Kyoto Encyclopedia of Genes and Genomes (KEGG) analysis, and Gene Ontology (GO) analysis. These were conducted using the *pheatmap*, *ggplot2*, *GseaVis*, and *clusterProfiler* R packages.

iPS cell culture and the induction of osteogenic differentiation

The iPS cell line was obtained from Ubigene (IPSC-DYR0100, China). Cells were seeded on plates coated with Matrigel® Matrix (356234, Corning, USA) and maintained in mTeSR® Plus medium (100-0276, STEMCELL, Canada), which supported their morphology and function. Passaging was performed once cells reached 80-90% confluence.

The osteogenic differentiation protocol was based on previously published methods [13]. Initially, cells were cultured in Dulbecco's Modified Eagle's Medium (DMEM) (11965092, Gibco, USA) supplemented with 10% fetal bovine serum (FBS) (A5670701, Gibco, USA). Upon reaching confluence, cells were switched to osteogenic medium (OM) containing DMEM, 2% FBS, $50\,\mu\text{g/ml}$ vitamin C (A103533, Aladdin, China), $10\,$ mM $\,\beta$ -glycerophosphate (G8100, Solarbio, China), and $10\,$ μM dexamethasone (D8040, Solarbio, China). Medium was refreshed every two days.

Reverse transcription quantitative PCR (RT-qPCR)

Total RNA was extracted using RNA isolation reagent (9108, Takara, Japan), and RNA concentration was measured. RNA was mixed with

Table 1. Primer sequences

Gene (Human)	Forward sequences (5' to 3')	Reverse sequences (5' to 3')
GAPDH	TGTTGCCATCAATGACCCCTT	CTCCACGACGTACTCAGCG
RUNX2	GCGCATTCCTCATCCCAGTA	GGCTCAGGTAGGAGGGGTAA
ALP	TTGTGCCAGAGAAAGAGAGAGA	GTTTCAGGGCATTTTTCAAGGT
NPY1R	GCAGGAGAAATACCAGCGGA	TCCCTTGAACTGAACAATCCTCTT
S0X2	CAGGAGTTGTCAAGGCAGAG	CCGCCGATGATTGTTATT

reverse transcriptase, oligo(dT) primers, and buffer, followed by incubation in a PCR amplifier for 15 minutes (R312, Vazyme, Nanjing, China). RT-qPCR was performed using cDNA, genespecific primers, and SYBR Green (R323, Vazyme, Nanjing, China). Primer sequences are listed in **Table 1**. Relative expression levels were calculated using the $2^{-\Delta\Delta CT}$ method.

Western blotting (WB)

Cell lysates were prepared using RIPA buffer (P0013B, Beyotime, China). Protein concentrations were measured with a BCA kit (P0010S, Beyotime, China). Equal amounts of protein were loaded onto 10% SDS-PAGE gels (PG112, Epizyme, China) and transferred onto PVDF membranes (ISEQ00010, Millipore, USA).

Membranes were blocked in TBST containing 5% BSA (37520, Thermo Fisher Scientific, USA) at room temperature for 1 hour. They were then incubated overnight at 4°C with primary antibodies (1:1000) targeting GAPDH (60004-1-Ig, Proteintech, China), ALP (MAB29092, R&D System, USA), RUNX2 (12556S, Cell Signaling Technology, USA), NPY1R (GB113733, Servicebio, China), AKT (200323-3B11, Zenbio, China), p-AKT (R381555, Zenbio, China), mTOR (222636, Zenbio, China), and p-mTOR (310302, Zenbio, China). After washing, membranes were incubated for 1 hour with a secondary antibody (31430, Thermo Fisher Scientific, USA) at a 1:5000 dilution. Bands were visualized using a chemiluminescence kit (34580, Thermo Fisher Scientific, USA) and quantified using ImageJ software.

Alkaline Phosphatase (ALP) staining and Alizarin Red Staining (ARS)

iPS cells were seeded on Matrigel®-coated plates and cultured in osteogenic medium containing small interfering RNA or inhibitors for 14

days. Cells were then washed with phosphate-buffered saline (PBS), fixed in paraformalde-hyde for 15 minutes, and rinsed three times with purified water. 1× Alizarin Red solution (ALIR-10001, OriCell, China) and ALP staining solution were added separately. After a 30-minute incubation, cells were rinsed again with purified water and imaged both grossly and under a microscope.

RNA interference (RNAi)

For siRNA transfection, cells were seeded to reach 70%-90% confluence. Lipofectamine™ 3000 reagent (L3000001, Invitrogen, USA) was diluted in Opti-MEM™ medium in two separate tubes and mixed well. A DNA master mix was prepared by diluting the DNA in Opti-MEM™ medium and adding P3000™ reagent. The DNA solution and Lipofectamine™ 3000 mixture were combined at a 1:1 ratio. The resulting DNA-lipid complexes were added to cells in 6-well or 12-well plates. Cells were incubated at 37°C for 2 to 4 days prior to downstream analysis.

Establishment of rat periodontitis model

This study was approved by the Ethics Committee of Guangxi Medical University (No. 202411003). Ten Sprague-Dawley (SD) rats (250-300 g) were purchased from the Guangxi Medical University Laboratory Animal Center (Guangxi, China) and acclimated for one week prior to experimental procedures. The rats were randomly assigned to two groups: control and periodontitis. Anesthesia was administered via intraperitoneal injection of 1% sodium pentobarbital at a dose of 5 mL/kg body weight. To induce periodontitis, the cervical region of the maxillary second molar was ligated using 0.2 mm stainless steel wire. On day 28 following induction, the rats were euthanized, and maxillae with attached soft tissues were harvested.

Micro-CT analysis

Alveolar bone loss and inflammatory effects on bone were assessed by Micro-CT scanning (Aloka Latheta LCT-200, Hitachi-Aloka). Three-dimensional reconstruction was carried out using Mimics Medical 21.0 software (Materialise, Belgium). The distance from the cemento-enamel junction (CEJ) to the alveolar bone crest (ABC) was measured with ImageJ software to quantify bone loss.

Hematoxylin and eosin (H&E) and Masson staining

After euthanasia, the maxillary tissues were excised and fixed in 4% paraformaldehyde at 4°C for 24 hours. The samples were then decalcified in 10% ethylenediaminetetraacetic acid (EDTA) solution (E1171, Solarbio, China). Following decalcification, tissues were dehydrated in graded ethanol (70%-100%), cleared with xylene, embedded in paraffin wax after three immersion cycles, and sectioned for histologic analysis.

H&E staining: Sections were deparaffinized with xylene, rehydrated through a graded ethanol series, and stained with hematoxylin for 10 minutes to visualize nuclei. After differentiation with ethanol hydrochloride, eosin staining was applied for 5 minutes to stain the cytoplasm. Slides were then dehydrated, cleared, and sealed with neutral gum.

Masson staining: Nuclei were stained with Wiegert's iron hematoxylin. Reich horn red acidic magenta was used for collagen fibers and myofibrils, followed by aniline blue staining for collagen fibrils after phosphomolybdic acid treatment. Slides were then dehydrated, cleared, and sealed. All stained sections were observed under a microscope.

Alizarin Red staining (ARS)

Paraffin sections of rat maxillae were deparaffinized with xylene and rehydrated through a graded ethanol series. Sections were then immersed in 0.1% Alizarin Red staining solution (pH 4.1-4.3) (G1038, Servicebio, China) and incubated at 37°C for 15 minutes. Following staining, sections were rinsed with distilled water, dehydrated with graded ethanol, cleared

with xylene, and sealed with neutral gum. Microscopic observation was then performed.

Immunohistochemistry (IHC) and Immunofluorescence (IF) staining

IHC staining: After antigen retrieval and blocking, maxillary sections were incubated overnight at 4°C with NPY1R primary antibody (1:200) (GB113733, Servicebio, China). The following day, sections were incubated with a secondary antibody at room temperature for 30 minutes and rinsed. Diaminobenzidine (DAB) was applied for color development. Hematoxylin was used for nuclear staining. Slides were then dehydrated, cleared, and sealed.

IF staining: Sections underwent antigen retrieval and blocking, followed by overnight incubation at 4°C with PI3K primary antibody (1:500) (GB11769, Servicebio, China) and mTOR primary antibody (1:200) (GB111839, Servicebio, China). The next day, a fluorescent secondary antibody was applied for 30 minutes. After rinsing with PBS, nuclei were counterstained with DAPI (C0065, Solarbio, China). Stained sections were observed under a fluorescence microscope.

Statistical analysis

Data were analyzed using IBM SPSS 23.0 software. Student's t-test was used to compare two groups when the data were normally distributed. For non-normally distributed data, the Mann-Whitney U test was applied. One-way ANOVA followed by the Tukey HSD test was used for comparisons among multiple groups. Differences were considered significant at P < 0.05.

Results

Identification of NPY/NPY1R and PI3K-Akt signaling in the osteogenic differentiation of iPS cells

To investigate the molecular mechanisms involved in the osteogenic differentiation of iPS cells, we analyzed the GSE219215 dataset retrieved from the Gene Expression Omnibus (GEO) database using bioinformatic approaches.

As shown in **Figure 1A**, the heatmap displays distinct clustering patterns of differentially

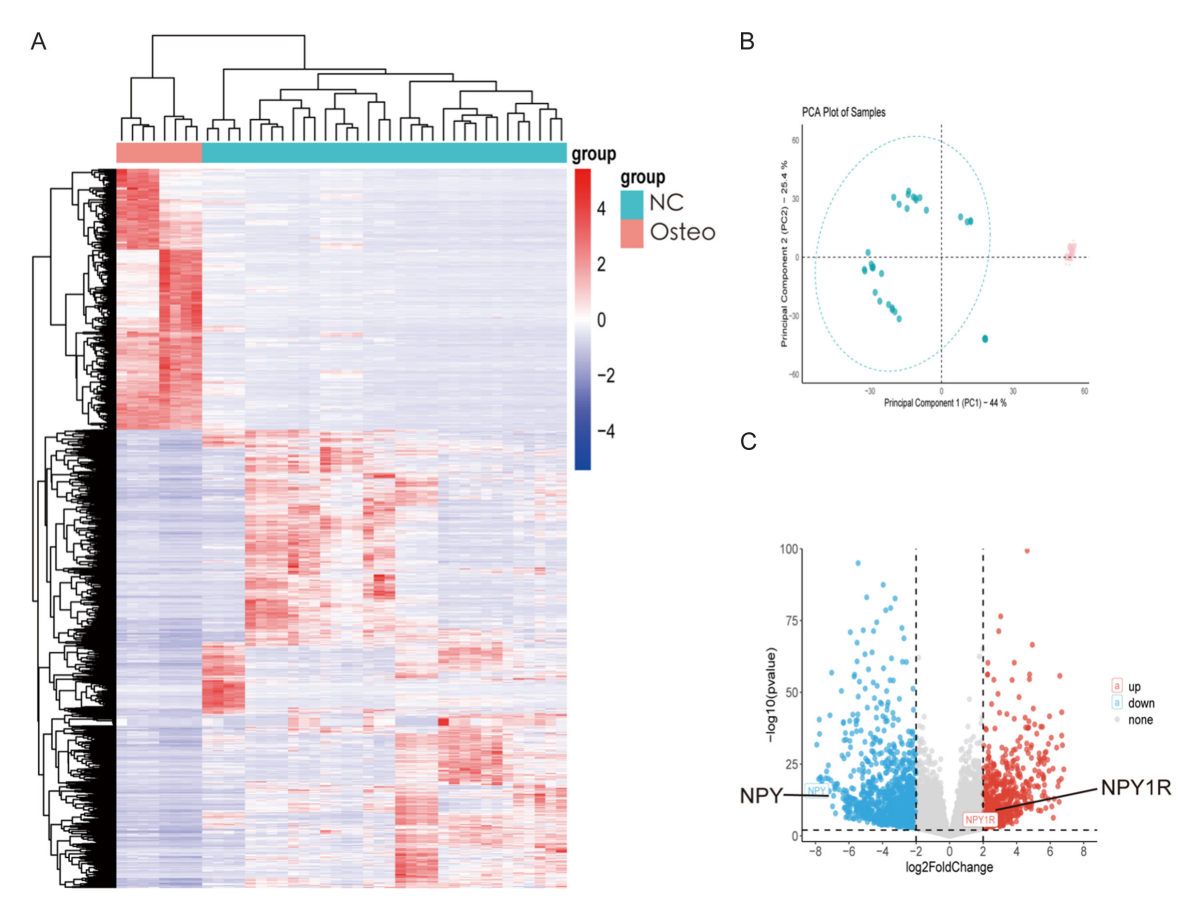


Figure 1. Transcriptomic analysis of gene expression changes during osteogenic differentiation of iPS cells. A. Heatmap showing hierarchical clustering of differentially expressed genes across all samples. B. Principal component analysis (PCA) illustrating separation between control and osteogenic differentiation groups. C. Volcano plot of differential gene expression; each point represents a single gene.

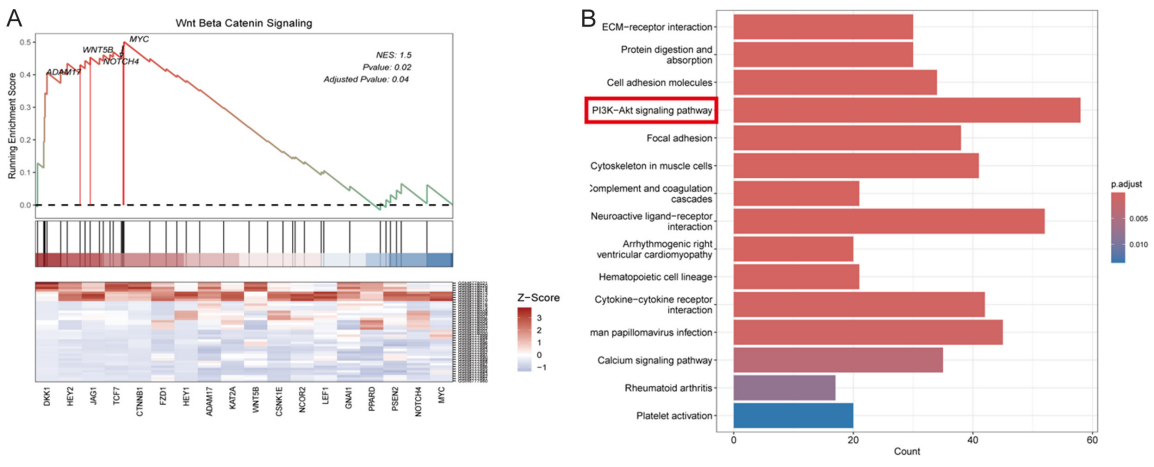
expressed genes between the control group and the osteogenic differentiation group. The PCA plot revealed clear separation between these two groups along the first two principal components (PC1 and PC2). Control samples clustered on the left, while osteogenic differentiation samples appeared on the right, indicating substantial differences in gene expression profiles (Figure 1B).

Volcano plot analysis identified 633 significantly upregulated and 1192 downregulated genes in the osteogenic differentiation group compared to the control. Among these, *NPY* and *NPY1R* exhibited notable fold changes with low *P* values, implying their involvement in osteogenic regulation. *NPY* was among the ten most significantly downregulated genes, whereas its receptor *NPY1R* showed significant upregulation during differentiation, with statistically meaningful differences (**Figure 1C**).

GSEA results indicate a significant enrichment of Wnt/ β -catenin pathway genes during osteogenic induction. The normalized enrichment score (NES) was 1.5, with an FDR-adjusted p value of 0.04. Considering the central role of the Wnt/ β -catenin pathway in calcification and osteogenesis [14], these findings suggest strong relevance to the osteogenic process (**Figure 2A**).

To identify the biological pathways associated with differentially expressed genes (DEGs), KEGG pathway enrichment analysis was conducted using the *ClusterProfiler* package, with a significance cutoff of *P* < 0.05. As shown in **Figure 2B**, the PI3K/AKT pathway exhibited the longest enrichment bar, indicating its strong association with the DEGs.

GO enrichment analysis was then performed to examine the distribution of DEGs across



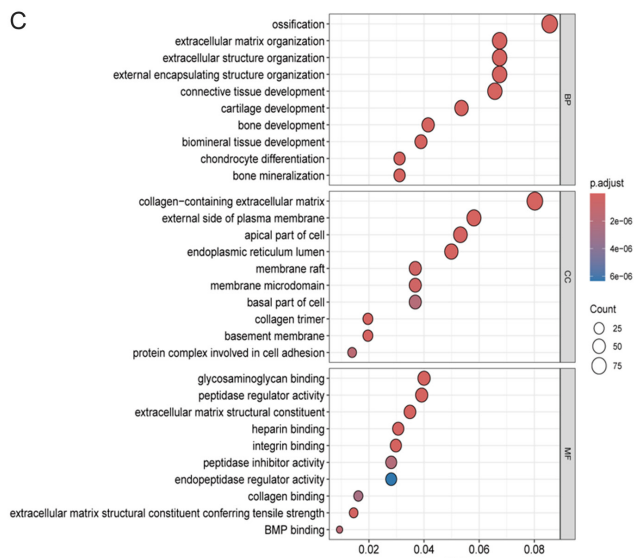


Figure 2. Analysis of the PI3K/AKT/mTOR signaling pathway during osteogenesis. A. Gene Set Enrichment Analysis (GSEA) plot showing enrichment of the Wnt/Bcatenin gene set in osteogenically differentiated iPS cells. The peak of the curve indicates the maximum enrichment score (ES), which is normalized (NES) to account for gene set size. P value and FDR q-value indicate statistical significance. B. KEGG pathway enrichment analysis identifying significantly enriched pathways (P < 0.05). C. GO analysis showing enriched biological processes (BP), cellular components (CC), and molecular functions (MF) during osteogenic differentiation.

biological processes, molecular functions, and cellular components. The results revealed significant enrichment in several GO categories. For Biological Process (BP), the term "osteogenesis" (GO:0001503) was enriched, with a p value of 0.0012. Within the Cellular Component (CC) category, genes were significantly enriched in the "extracellular matrix containing collagen" (GO:00062023), with a p value of 0.0010. These findings suggest that the identified DEGs are closely linked to bone formation and extracellular matrix organization (Figure 2C).

Together, these results point to critical molecular signatures involving NPY/NPY1R and the PI3K/AKT-mTOR pathway that may drive the osteogenic differentiation of iPS cells and contribute to alveolar bone development. These pathways may also serve as useful

biomarkers in the context of bone-related disorders.

Role of NPY1R in osteogenic differentiation of iPSCs

To investigate the role of NPY1R in the osteogenic differentiation of iPSCs, we used an *in vitro* model and carried out a series of molecular and functional experiments.

Osteogenic differentiation was initiated by culturing iPSCs in osteogenic medium (OM) for a defined period, as shown in **Figure 3A**. Light microscopy revealed morphologic changes consistent with osteoblast lineage differentiation, with cells displaying a more elongated shape following induction (**Figure 3B**).

RT-qPCR results (**Figure 3C-F**) showed significant upregulation of osteogenic markers,

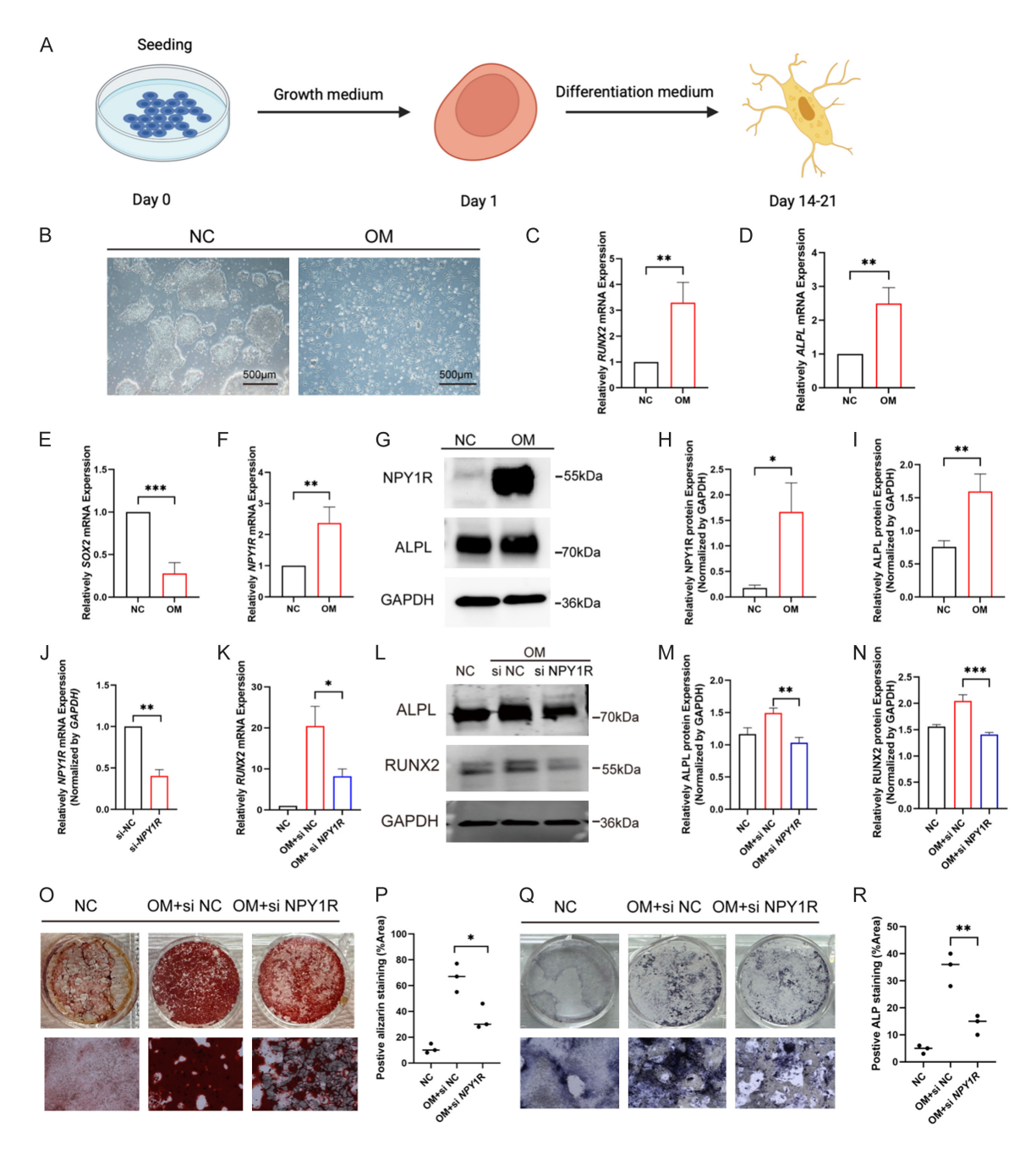


Figure 3. Role of NPY1R in iPS cells before and after *in vitro* osteogenic differentiation. A. Schematic illustration of the iPSC osteogenic differentiation process. B. Microscopic images of iPS cells before and after osteogenic induction. C-F. RT-qPCR analysis showing relative mRNA expression of RUNX2, ALPL, SOX2, and NPY1R before and after osteogenic differentiation. G-I. Western blot and quantification of NPY1R and ALPL protein expression before and after differentiation. J. RT-qPCR analysis of NPY1R mRNA expression in iPS cells with or without NPY1R knockdown. K. RT-qPCR analysis of RUNX2 mRNA expression in cells with or without NPY1R knockdown. L-N. Western blot and quantification of RUNX2 and ALPL protein levels in NPY1R-knockdown vs. control cells. O, P. Alizarin Red staining and quantification to assess mineralization in cells with or without NPY1R knockdown. Q, R. ALP staining and quantification to evaluate alkaline phosphatase activity under the same conditions. Data are presented as mean \pm SD, n = 3. *: P < 0.05, **: P < 0.01, ***: P < 0.001.

including *RUNX2* and *ALPL*, and downregulation of pluripotency markers such as *SOX2*. Notably, *NPY1R* expression was markedly

increased during differentiation, suggesting its involvement in osteogenic regulation. These transcriptional changes were further supported

by wblotting (**Figure 3G-I**), which demonstrated elevated protein levels of ALPL and NPY1R after induction.

To examine the functional role of NPY1R, siRNA was used to knock down its expression in iPSCs. RT-qPCR confirmed successful knockdown, with a substantial decrease in NPY1R mRNA levels (Figure 3J). Analysis of RUNX2 expression in NPY1R-silenced cells (Figure 3K) showed a significant reduction, indicating a possible regulatory relationship between NPY1R and RUNX2 during osteogenesis.

Western blotting further revealed decreased protein levels of RUNX2 and ALPL in NPY1R-knockdown cells cultured in osteogenic medium (**Figure 3L-N**), reinforcing the conclusion that NPY1R contributes to the osteogenic program.

Functionally, Alizarin Red staining showed reduced mineral deposition in NPY1R-silenced iPSCs compared to controls, highlighting the importance of NPY1R in matrix mineralization (Figure 30, 3P). Similarly, ALP staining indicated reduced alkaline phosphatase activity in NPY1R-deficient cells (Figure 3Q, 3R), consistent with impaired osteogenic differentiation.

Together, these findings demonstrate that NPY1R plays a central role in the osteogenic differentiation of iPSCs, affecting both gene and protein expression profiles and functional markers of osteoblast maturation.

Connection between NPY1R and osteogenesis-related PI3K/AKT/mTOR pathway of iPSCs

To explore the involvement of the PI3K/AKT/mTOR signaling pathway in osteogenic differentiation, we employed iPSCs as an *in vitro* model. Western blot analysis of iPSCs cultured in osteogenic medium (OM) revealed increased phosphorylation of AKT (p-AKT) and mTOR (p-mTOR), indicating activation of the PI3K/AKT/mTOR pathway during differentiation (Figure 4B-D).

The effect of PI3K inhibition on osteogenesis was assessed using RT-qPCR. Treatment with LY294002 led to a significant reduction in *RUNX2* and *ALPL* mRNA levels, two key osteogenic markers, compared to the control group (**Figure 4E**, **4F**). Western blot results aligned with these findings, showing decreased

protein expression of RUNX2 and ALPL in LY294002-treated iPSCs cultured in OM (**Figure 4G-I**).

To examine the functional outcome of PI3K/AKT pathway inhibition, ARS and ALP staining were performed. Both assays revealed a clear reduction in mineralized matrix formation and alkaline phosphatase activity in LY294002-treated cells, compared to untreated controls (Figure 4J-M). These results confirm that blocking the PI3K/AKT/mTOR pathway impairs osteogenic differentiation in iPSCs, highlighting its importance in this process.

Further, we analyzed the phosphorylation status of AKT following *NPY1R* knockdown using western blotting (**Figure 4N**, **40**). Silencing *NPY1R* resulted in decreased levels of p-AKT, suggesting that NPY1R influences activation of the PI3K/AKT pathway.

ARS staining revealed that exogenous NPY significantly increased calcium deposition, indicating promoted osteogenesis (**Figure 4P**, **4Q**). However, when co-treated with the PI3K inhibitor LY294002, this effect was significantly reduced, suggesting that the pro-osteogenic function of NPY depends on the activation of the PAM pathway.

These findings offer functional evidence that the PAM pathway plays a central role in mediating the effects of NPY during osteogenic differentiation. Together, the results suggest that PI3K/AKT signaling may act downstream of NPY1R to regulate osteogenic outcomes in iPSCs (Figure 4A).

Evaluation of in vivo bone loss in the rat periodontitis model

Building on the *in vitro* results, we next examined whether the roles of NPY1R and the PI3K/AKT/mTOR pathway in osteogenic differentiation could be confirmed *in vivo*, within the complex physiological environment. To evaluate their relevance to bone loss, we used a ligature-induced periodontitis (LIP) rat model, which effectively replicates the pathological features of periodontal disease and bone resorption. This approach allowed us to determine whether the effects observed *in vitro* translate to a physiologically relevant *in vivo* setting.

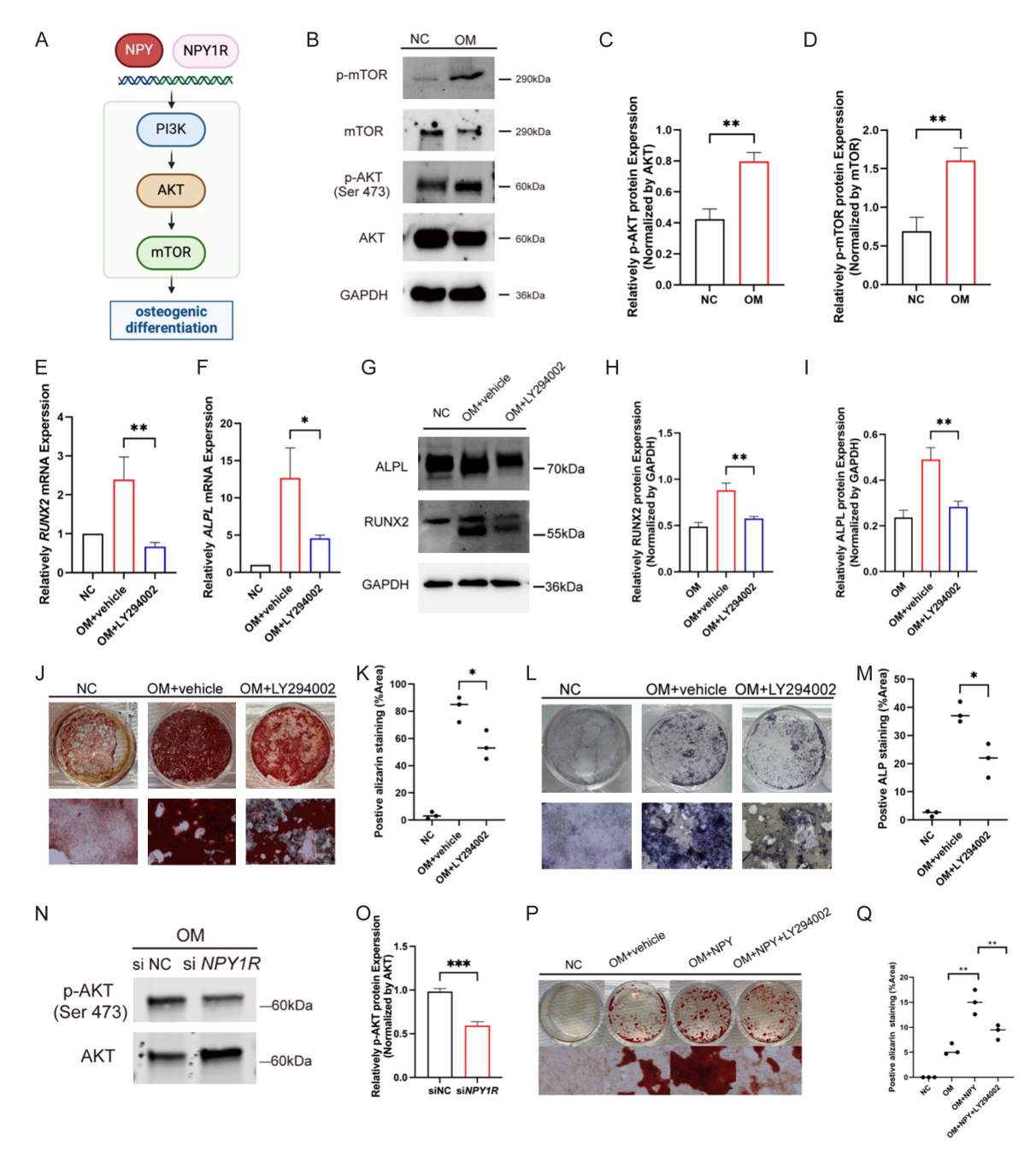


Figure 4. Activity of the PI3K/AKT/mTOR signaling pathway in iPS cells during osteogenic differentiation and its connection with NPY1R. A. Schematic overview of the investigation into PI3K/AKT/mTOR pathway activity and its relationship with NPY1R during osteogenesis. B-D. Western blot analysis and quantification of p-AKT/AKT and p-mTOR/mTOR protein levels in iPS cells before and after osteogenic differentiation. E, F. RT-qPCR analysis of *RUNX2* and *ALPL* mRNA expression in iPS cells with or without the PI3K inhibitor LY294002. G-I. Western blot and quantification of RUNX2 and ALPL protein levels under LY294002 treatment. J, K. Alizarin Red staining and quantification of mineral deposition in iPS cells treated with or without LY294002. L, M. ALP staining and quantification of alkaline phosphatase activity under the same conditions. N, O. Western blot and quantification of p-AKT and AKT protein expression in iPS cells with or without NPY1R knockdown. P, Q. Alizarin Red staining and quantification of mineral deposition in iPS cells treated with or without NPY+LY294002. Data are presented as mean \pm SD, n = 3. *: P < 0.05, **: P < 0.01, ***: P < 0.001.

To induce periodontitis, stainless steel wire was used to ligate the maxillary second molar,

establishing the rat model (**Figure 5A**). Both 2D and 3D micro-CT images revealed significant

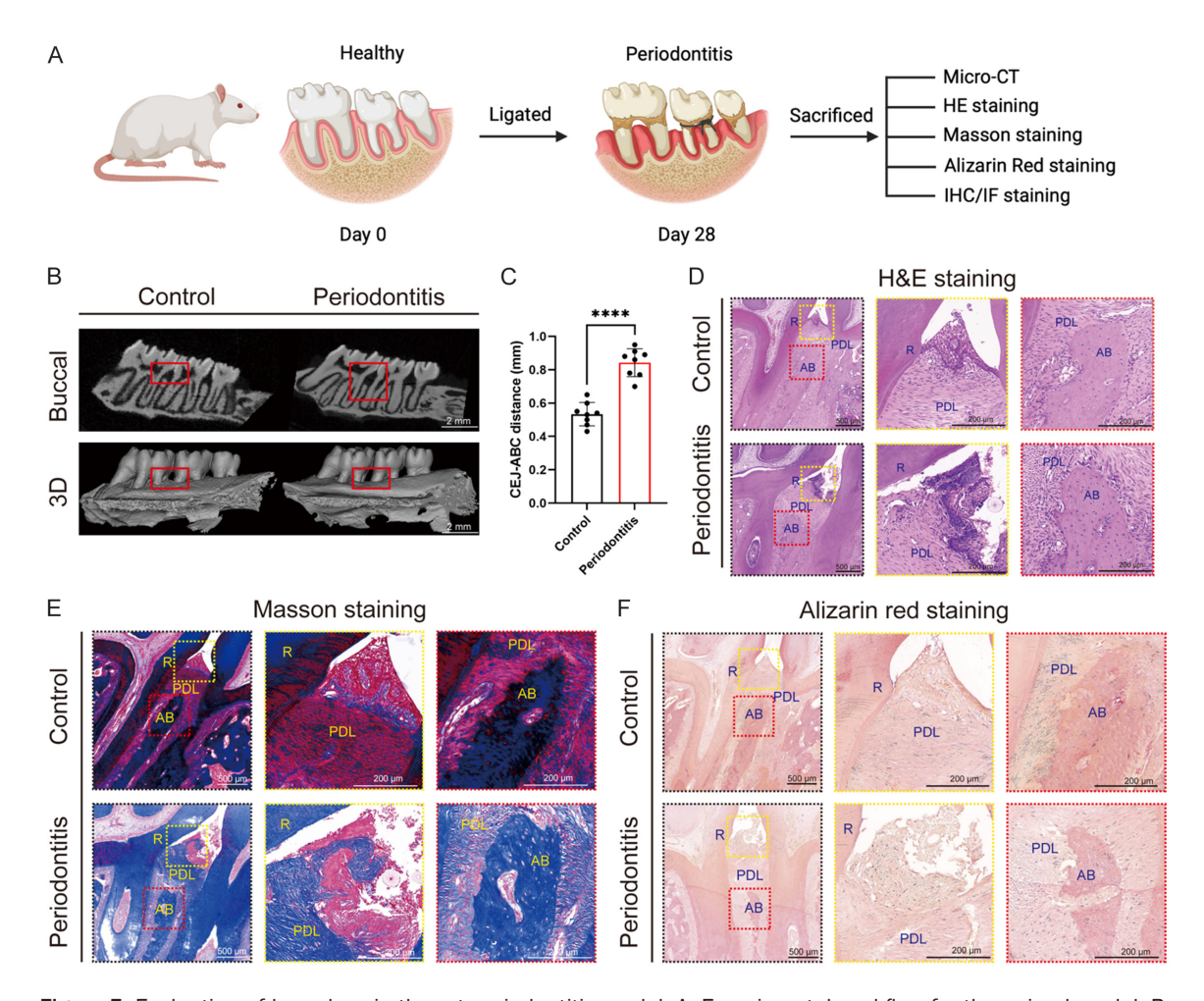


Figure 5. Evaluation of bone loss in the rat periodontitis model. A. Experimental workflow for the animal model. B. 2D and 3D micro-CT images of maxillary bone structures from control and periodontitis groups. C. Quantification of CEJ-ABC distance. D. H&E staining of maxillary sections showing bone architecture. E. Masson staining to assess collagen fiber organization. F. Alizarin Red staining of mineralized tissue in maxillae. R: root, PDL: periodontal ligament, AB: alveolar bone. Data are presented as mean \pm SD, n = 8. ****: P < 0.0001.

differences in maxillary bone morphology between the control and periodontitis groups (Figure 5B). Measurement of the cementoenamel junction to alveolar bone crest (CEJ-ABC) distance, a key indicator of bone resorption, showed a significant increase in the periodontitis group, reflecting greater bone loss (Figure 5C).

Histologic staining provided further confirmation of structural and compositional differences. H&E staining demonstrated notable disruption of bone architecture in the periodontitis group, in contrast to the preserved structure seen in controls (Figure 5D). Masson staining showed that collagen fibers in the control group were well-aligned and uniformly distributed, while those in the periodontitis group appeared

irregular and disorganized (**Figure 5E**). In addition, Alizarin Red staining (ARS) revealed decreased mineral deposition in the periodontitis group, indicating reduced bone density (**Figure 5F**).

NPY1R expression and the PI3K/AKT/mTOR pathway in rat model of periodontitis

IHC and IF were used to examine NPY1R expression and the activation of key components of the PI3K/AKT/mTOR pathway in the periodontal tissues of rats with experimentally-induced periodontitis.

As shown in **Figure 6A**, representative IHC images revealed a clear upregulation of NPY1R in the periodontal tissues of the periodontitis

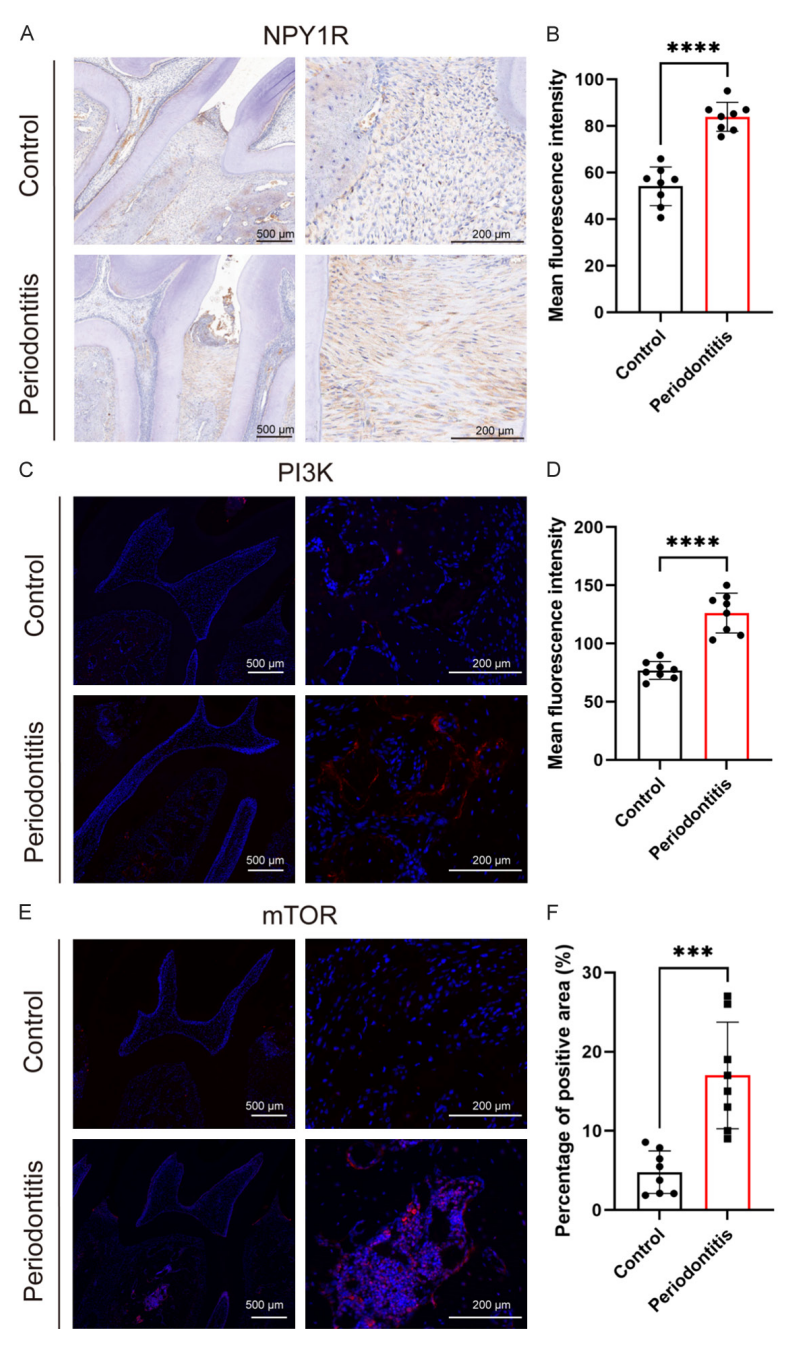


Figure 6. Expression of NPY1R, PI3K, and mTOR in rat alveolar bone. A, B. IHC staining and quantification of NPY1R expression. C, D. IF staining and quantification of PI3K. E, F. IF staining and quantification of mTOR. Data are presented as mean \pm SD, n = 8. ***: P < 0.001, ****: P < 0.0001.

group compared to the control group. Quantitative analysis confirmed a significant increase in NPY1R expression in the periodontitis group (P < 0.05) (Figure 6B).

We further assessed the activation of the PI3K/AKT/mTOR pathway. Immunofluorescent

staining of PI3K (**Figure 6C**) and mTOR (**Figure 6E**) showed strong fluorescence signals in the periodontal tissues of rats with periodontitis, suggesting elevated activity. Quantification of these signals confirmed significantly higher expression levels of PI3K (**Figure 6D**) and mTOR (**Figure 6F**) in the periodontitis group, including noticeable nuclear aggregation (*P* < 0.05).

These findings suggest that the PI3K/AKT/mTOR pathway is activated in response to periodontitis and may be regulated through NPY1R expression, pointing to a potential mechanistic link in the disease process.

Discussion

Periodontitis-related bone defects remain a leading cause of tooth loss in adults, with millions of cases worldwide linked to alveolar bone destruction each year [15]. Although several studies have described a genetic basis of the disease [16-19], translating these findings into clinical treatments has proven challenging. To date, there are still no widely effective drugs specifically developed for the treatment of human alveolar bone loss [20], creating a pressing need to better understand the disease mechanism.

In this study, we provide clear evidence that *NPY1R* and the PI3K/AKT/mTOR signaling pa-

thway are involved in osteogenic differentiation and bone loss, based on results from both *in vitro* and *in vivo* models. Our findings reflect the complexity of molecular regulation in osteogenesis and bone resorption during periodontitis. Through a combined approach involving bioinformatics, molecular biology, and

histologic analysis, we identified key signaling events that influence bone remodeling in the disease context. These results point to potential targets for addressing bone loss in periodontitis and related conditions.

Our observations are consistent with previous reports showing that the NPY/NPY1R system plays a role in promoting osteogenesis [21, 22]. This raises the possibility of targeting this pathway to support bone formation, both in the context of fracture repair and in preventing alveolar bone loss in patients with periodontitis. Interestingly, transcriptomic data in our study showed marked downregulation of the NPY ligand gene and a concurrent upregulation of its receptor NPY1R during iPSC osteogenic differentiation. These results align with earlier findings. Igwe reported that NPY expressed by osteocytes can suppress osteoblast activity [23], which contrasts with the action of classical NPY produced by the nervous system and transported to bone tissue. This discrepancy may explain the downregulation of NPY and upregulation of NPY1R observed in our iPSC model, pointing to a nuanced, context-dependent role of this signaling axis during bone formation.

In addition, this is not the first report suggesting that the PI3K/AKT/mTOR signaling pathway may act downstream of NPY/NPY1R. Zhou found that NPY can induce TGF-β1 production in RAW264.7 cells through the Y1 receptor, and that this effect may involve activation of the PI3K pathway [24]. In our iPSC osteogenic differentiation model, the AKT phosphorylation site identified was Ser473, which is downstream of the mTOR pathway [25]. This observation corresponds with the elevated phosphorylation of mTOR detected in our study. Taken together, these consistent results strengthen the reliability of the findings presented here.

We recognize that iPSC-derived osteogenesis models primarily follow the endochondral ossification route and may not fully capture the intramembranous ossification process typical of alveolar bone. Our use of iPSCs was guided by their pluripotency and reproducibility, which make them a practical system for mechanistic exploration. However, we acknowledge that oral-derived stem cells, such as dental pulp stem cells (DPSCs) and periodontal ligament stem cells (PDLSCs), more closely represent

the native environment of alveolar bone regeneration. In future work, we plan to extend our validation using these oral-specific stem cells to increase the physiological relevance of our findings.

Notably, our observation of increased NPY1R expression in a rat model of periodontitis contrasts with the findings of Lundy, who reported downregulation of NPY1R in human periodontitis tissue [26]. One possible explanation is that Lundy's samples were collected from patients with periodontitis, but not necessarily from those with advanced alveolar bone destruction. Different stages or severities of the disease may exhibit distinct molecular profiles due to complex gene regulation and possible compensatory mechanisms. Moreover, most previous studies have concentrated on the role of NPY and NPY1R in inflammation, without exploring the signaling mechanisms that influence osteogenesis. Therefore, the differences between our findings and earlier reports do not weaken the conclusions of this study.

Our findings carry meaningful clinical implications for the treatment of periodontitis and other bone-related disorders. Prior research has shown that interventions targeting the nervous system can reduce bone loss in periodontitis [27], and since NPY is secreted by the nervous system, it is reasonable to consider its involvement in these therapeutic effects. Targeting the NPY1R and PI3K/AKT/mTOR signaling pathways may offer new strategies for preventing or reducing bone loss in conditions such as periodontitis, osteoporosis, and other inflammatory bone diseases. By adjusting these pathways, it may be possible to restore the balance between osteoclast and osteoblast activity, improving bone regeneration and repair. In particular, activation of the PI3K/AKT/ mTOR pathway could support osteoblast differentiation and mineral deposition, while limiting excessive osteoclast activity may help reduce bone resorption.

The therapeutic use of these pathways could also be applied to regenerative medicine and bone tissue engineering. Future research should aim to examine the long-term effects of modifying NPY1R and PI3K/AKT/mTOR signaling *in vivo*, using both pharmacologic inhibitors and gene-editing tools to clarify their

roles in bone repair and remodeling. One method involves the administration of exogenous NPY, which is a relatively straightforward approach with promise for clinical translation [28, 29].

A limitation of this study lies in the use of a cellular model based on iPSCs undergoing endochondral osteogenesis, a process more commonly linked to long bone development [30]. In contrast, alveolar bone mainly forms through intramembranous ossification [31]. However, validation of NPY1R's role using an animal model of alveolar bone loss helps to address this limitation.

Conclusions

This study systematically investigated the molecular pathways involved in osteogenic differentiation and bone loss associated with periodontitis. The observed upregulation of NPY1R and activation of the PI3K/AKT/mTOR pathway in both *in vitro* and *in vivo* models highlights the importance of these signaling routes in bone remodeling. These insights have therapeutic implications for treating periodontal disease and other disorders involving bone loss.

Acknowledgements

This research was funded by Joint Project on Regional High-Incidence Diseases Research of Guangxi Natural Science Foundation (Grant number: 2025GXNSFAA069603), Guangxi medical and health appropriate technology development and application project (Grant number: S2021084), Fundamental Research Funds for the Central Universities of Central South University (Grant number: 2023ZZTS0208), and Hunan Provincial Innovation Foundation for Postgraduate (Grant number: CX20230284). We thank BioRender for providing the online tool used to create the figures in this study. Related figures are used with permission.

Disclosure of conflict of interest

None.

Address correspondence to: Xiaojie Li, Guangxi Key Laboratory of Oral and Maxillofacial Rehabilitation and Reconstruction, College and Hospital of Stomatology, Guangxi Medical University, No. 22 Shuangyong Road, Nanning 530021, Guangxi, P. R. China. E-mail: KQ100448@sr.gxmu.edu.cn; Zhen Qi, Department of Cardiovascular Surgery, The Second Xiangya Hospital, Central South University, No. 136 Middle Renmin Road, Changsha 410000, Hunan, P. R. China. E-mail: 228202110@csu.edu.cn

References

- [1] Nascimento GG, Alves-Costa S and Romandini M. Burden of severe periodontitis and edentulism in 2021, with projections up to 2050: the global burden of disease 2021 study. J Periodontal Res 2024; 59: 823-867.
- [2] Wang H, Divaris K, Pan B, Li X, Lim JH, Saha G, Barovic M, Giannakou D, Korostoff JM, Bing Y, Sen S, Moss K, Wu D, Beck JD, Ballantyne CM, Natarajan P, North KE, Netea MG, Chavakis T and Hajishengallis G. Clonal hematopoiesis driven by mutated DNMT3A promotes inflammatory bone loss. Cell 2024; 187: 3690-3711, e3619.
- [3] Ogawa H, McKenna G and Kettratad-Pruksapong M. Prevention of oral functional decline. Int Dent J 2022; 72: S21-S26.
- [4] Preshaw PM, Alba AL, Herrera D, Jepsen S, Konstantinidis A, Makrilakis K and Taylor R. Periodontitis and diabetes: a two-way relationship. Diabetologia 2012; 55: 21-31.
- [5] Tonetti MS. Dental pathophysiology of odontogenic sinusitis: periodontitis. Otolaryngol Clin North Am 2024; 57: 957-975.
- [6] Luo X, Wan Q, Cheng L and Xu R. Mechanisms of bone remodeling and therapeutic strategies in chronic apical periodontitis. Front Cell Infect Microbiol 2022; 12: 908859.
- [7] Augustine R, Gezek M, Nikolopoulos VK, Buck PL, Bostanci NS and Camci-Unal G. Stem cells in bone tissue engineering: progress, promises and challenges. Stem Cell Rev Rep 2024; 20: 1692-1731.
- [8] Shi YC and Baldock PA. Central and peripheral mechanisms of the NPY system in the regulation of bone and adipose tissue. Bone 2012; 50: 430-436.
- [9] Chen QC and Zhang Y. The role of NPY in the regulation of bone metabolism. Front Endocrinol (Lausanne) 2022; 13: 833485.
- [10] Lamande SR, Ng ES, Cameron TL, Kung LHW, Sampurno L, Rowley L, Lilianty J, Patria YN, Stenta T, Hanssen E, Bell KM, Saxena R, Stok KS, Stanley EG, Elefanty AG and Bateman JF. Modeling human skeletal development using human pluripotent stem cells. Proc Natl Acad Sci U S A 2023; 120: e2211510120.
- [11] Lay AC, Barrington AF, Hurcombe JA, Ramnath RD, Graham M, Lewis PA, Wilson MC, Heesom KJ, Butler MJ, Perrett RM, Neal CR, Herbert E, Mountjoy E, Atan D, Nair V, Ju W, Nelson RG, Kretzler M, Satchell SC, McArdle CA, Welsh GI

- and Coward RJM. A role for NPY-NPY2R signaling in albuminuric kidney disease. Proc Natl Acad Sci U S A 2020; 117: 15862-15873.
- [12] Chai S, Yang Y, Wei L, Cao Y, Ma J, Zheng X, Teng J and Qin N. Luteolin rescues postmenopausal osteoporosis elicited by OVX through alleviating osteoblast pyroptosis via activating PI3K-AKT signaling. Phytomedicine 2024; 128: 155516.
- [13] Okamura K, Inagaki Y, Matsui TK, Matsubayashi M, Komeda T, Ogawa M, Mori E and Tanaka Y. RT-qPCR analyses on the osteogenic differentiation from human iPS cells: an investigation of reference genes. Sci Rep 2020; 10: 11748.
- [14] Baron R and Kneissel M. WNT signaling in bone homeostasis and disease: from human mutations to treatments. Nat Med 2013; 19: 179-192.
- [15] Slots J. Periodontitis: facts, fallacies and the future. Periodontol 2000 2017; 75: 7-23.
- [16] Fan Y, Cui C, Rosen CJ, Sato T, Xu R, Li P, Wei X, Bi R, Yuan Q and Zhou C. Klotho in Osx(+)mesenchymal progenitors exerts pro-osteogenic and anti-inflammatory effects during mandibular alveolar bone formation and repair. Signal Transduct Target Ther 2022; 7: 155.
- [17] Jovanovic SA, Hunt DR, Bernard GW, Spiekermann H, Wozney JM and Wikesjo UM. Bone reconstruction following implantation of rh-BMP-2 and guided bone regeneration in canine alveolar ridge defects. Clin Oral Implants Res 2007; 18: 224-230.
- [18] Liu Y, Li Z, Arioka M, Wang L, Bao C and Helms JA. WNT3A accelerates delayed alveolar bone repair in ovariectomized mice. Osteoporos Int 2019; 30: 1873-1885.
- [19] Chen Y, Weng Y, Huang J, Li Q, Sun B, Wang H and Wang Z. Leptin receptor (+) stromal cells respond to periodontitis and attenuate alveolar bone repair via CCRL2-mediated Wnt inhibition. J Bone Miner Res 2024; 39: 611-626.
- [20] Kim KA, Choi EK, Ohe JY, Ahn HW and Kim SJ. Effect of low-level laser therapy on orthodontic tooth movement into bone-grafted alveolar defects. Am J Orthod Dentofacial Orthop 2015; 148: 608-617.

- [21] Dong P, Gu X, Zhu G, Li M, Ma B and Zi Y. Melatonin induces osteoblastic differentiation of mesenchymal stem cells and promotes fracture healing in a rat model of femoral fracture via neuropeptide Y/neuropeptide y receptor Y1 signaling. Pharmacology 2018; 102: 272-280.
- [22] Xie W, Han Y, Li F, Gu X, Su D, Yu W, Li Z and Xiao J. Neuropeptide Y1 receptor antagonist alters gut microbiota and alleviates the ovariectomy-induced osteoporosis in rats. Calcif Tissue Int 2020; 106: 444-454.
- [23] Igwe JC, Jiang X, Paic F, Ma L, Adams DJ, Baldock PA, Pilbeam CC and Kalajzic I. Neuropeptide Y is expressed by osteocytes and can inhibit osteoblastic activity. J Cell Biochem 2009; 108: 621-630.
- [24] Zhou JR, Xu Z and Jiang CL. Neuropeptide Y promotes TGF-beta1 production in RAW264.7 cells by activating PI3K pathway via Y1 receptor. Neurosci Bull 2008; 24: 155-159.
- [25] Gough NR. Focus issue: TOR signaling, a tale of two complexes. Sci Signal 2012; 5: eg4.
- [26] Lundy FT, El Karim IA and Linden GJ. Neuropeptide Y (NPY) and NPY Y1 receptor in periodontal health and disease. Arch Oral Biol 2009; 54: 258-262.
- [27] Ribeiro AB, Brognara F, da Silva JF, Castania JA, Fernandes PG, Tostes RC and Salgado HC. Carotid sinus nerve stimulation attenuates alveolar bone loss and inflammation in experimental periodontitis. Sci Rep 2020; 10: 19258.
- [28] Brod SA and Bauer VL. Ingested (oral) neuropeptide Y inhibits EAE. J Neuroimmunol 2012; 250: 44-49.
- [29] Bose M, Farias Quipildor G, Ehrlich ME and Salton SR. Intranasal peptide therapeutics: a promising avenue for overcoming the challenges of traditional CNS drug development. Cells 2022; 11: 3629.
- [30] Saul D and Khosla S. Fracture healing in the setting of endocrine diseases, aging, and cellular senescence. Endocr Rev 2022; 43: 984-1002.
- [31] Salhotra A, Shah HN, Levi B and Longaker MT. Mechanisms of bone development and repair. Nat Rev Mol Cell Biol 2020; 21: 696-711.